Efficient On-Board Charger to Improve the Life Time of Electric Vehicle Battery

Swathi Karike
Department of Electrical and Electronics Engineering, Koneru Lakshmaiah Education Foundation, India
swathikarikephd@gmail.com (corresponding author)

Kuthuri Narasimha Raju
Department of Electrical and Electronics Engineering, Koneru Lakshmaiah Education Foundation, India
narasimharaju_eee@kluniversity.in

Sudha Rani Donepudi
Department of Electrical and Electronics Engineering, Sri Vasavi Engineering College, India
lakshmisudha124@gmail.com

Received: 20 February 2024 | Revised: 18 March 2024 | Accepted: 3 April 2024

 DOI: https://doi.org/10.48084/etasr.7111

ABSTRACT

Internal combustion engines produce about 10% of the world's greenhouse gas emissions. Electric vehicles generate 17-30% lower emissions than the internal combustion engines. However, the formers entail certain drawbacks, namely the few available charging stations, the high charging cost, and the limited battery life. The purpose of this paper is to propose the best suitable converter for the on-board charger, which will be able to decrease the charging cost by improving the power factor and the battery life span. This enhancement will be accomplished through the reduction of the charging current either at a very high or very low State of Charge (SOC). Isolated and non-isolated converter topologies were studied to identify the most suitable converter for the on-board charger that will be able to ameliorate the efficiency and the input power factor as well as control the charging current limits. A non-isolated buck converter with switched inductors is used for the power factor adjustment along with the current control approach to achieve a highly efficient on-board charger. Compared to the isolated converter with transformers, the non-isolated hybrid switched inductor buck converter has a wider current control range. MATLAB/Simulink output results were analyzed to validate the performance of the designed on-board charger with a non-isolated converter.

Keywords-EV charger; non-isolated converter; power factor correction; input and output current control; on-board charger

I. INTRODUCTION

Electric Vehicles (EVs) act as a solution for the elimination of fuel consumption. However, they are not yet extensively used. To achieve a wide spread utilization of EVs in the future, many challenges have to be overcome. One of the primary difficulties is the establishment of an extensive and efficient charging infrastructure. This includes both public charging stations and home charging solutions. The availability of charging stations, especially in regions with lower EV adoption rates, can significantly impact the convenience and feasibility of owning an electric vehicle. Charging an EV typically takes longer than refueling a traditional gasoline internal combustion vehicle. Fast charging technologies have improved this type of delay, but challenges still remain in terms of the charging speeds, especially for longer-range EVs. Balancing charging speed with battery longevity and safety is also a consideration. On-board chargers are an alternative solution for the charging stations. Traditional on-board EV battery chargers as shown in Figure 1 are utilized to charge E batteries deploying isolated converters with built-in transformers, along with a voltage conversion isolation transformer employed to maintain safety. Traditional isolated chargers consist of two stage operations. In the first stage the rectifier used for Power Factor Correction (PFC) and in the second stage an isolated converter with coupled inductors is implemented for dc-to-dc voltage conversion [1-2]. The power factor rectifier regulates the input ac current while controlling the output dc voltage to maintain low total harmonic distortion and the sinusoidal shape as the input ac voltage [3]. In the isolated converter, input ac current ripples can be filtered by bulky coupled inductors. As the PFC rectifier already provides the constant dc output voltage, the dc-to-dc stage operates on isolated voltage with the help of a transformer [4-5]. Because of the two-stage function, isolated converters suffer from increased charging cost and less efficiency. The charger plays an important role in battery life

and vehicle performance. Discharging and charging are two unavoidable battery aging situations in EV applications. Irregular charging of the battery impacts the performance and battery life time, especially at very low and very high SOC. They deteriorate cell chemistry and reduce the life span of the EV battery [6-7]. Degradation of the battery can be identified with the State of Life (SOL). Internal resistance is a health indicator of a battery, and SOL is derived as:

$$SOL_{Rbased} = \frac{R_{EOL}(SOC,T) - R_{ACT}(SOC,T)}{R_{EOL}(SOC,T) - R_{BOL}(SOC,T)} \times 100\% \quad (1)$$

where $R_{ACT}(SOC, T)$ is the actual internal resistance, $R_{BOL}(SOC, T)$ is the initial internal resistance of the battery, and $R_{EOL}(SOC, T)$ is the internal resistance of the battery at the end of its life at given SOC and temperature conditions. Equation (1) indicates that battery aging increases while charging the battery under high and low SOC conditions [8-11]. Conventional isolated converters with fixed turns ratio cannot control the charging current for a SOC lower than 20% or higher than 80%.

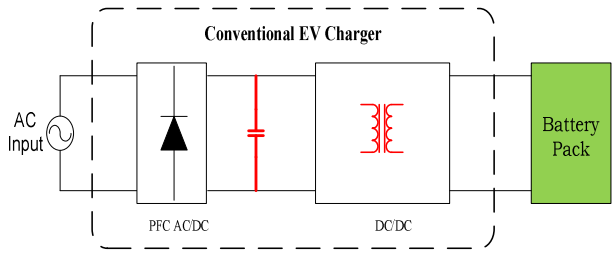

Fig. 1. Charger with isolated dc/dc converter.

To overcome the aforementioned challenges, the high power factor and a more efficient non-isolated converter with a switched inductor buck converter are proposed to be used in an on-board charger application. Figure 2 depicts the recommended isolated converter with an input EMI strain filter, a diode bridge rectifier, and a switched inductor buck converter [12-15]. The utilization of the switched inductor reduces bulky and large sized coupled inductors/transformers.

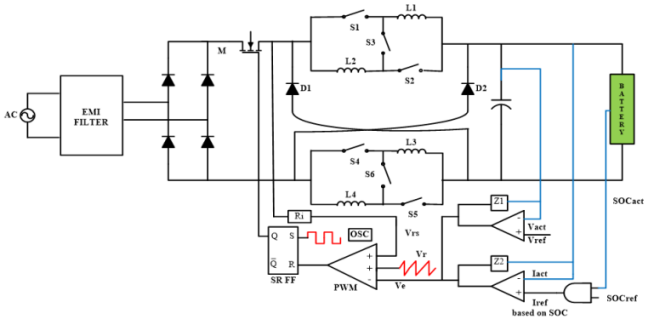

Fig. 2. The proposed non-isolated switched inductor buck converter.

II. SWITCHED INDUCTOR WITH HYBRID BUCK TOPOLOGY

A variation of the traditional buck topology, the switch inductor hybrid buck topology, has four inductors and two diodes with one main switch (M) enabling the appropriate current direction flow, which divides the inductance in four parts (L_1, L_2, L_3, and L_4). Authors in [1] used coupled inductors, but this work utilizes isolated inductors to reduce size [16]. The particular work switched the four inductors with six switches ($S_1 - S_6$) functioning just in DCM for increased efficiency as it permits ZCS and eliminates reverse recovery loss [17-18]. Additionally, lower inductance is possible with DCM operation, increasing total power density. Figure3 illustrates the current direction flow through each operating stage of the switching inductor buck converter PFC design. The individual inductors were considered to be equal, i.e. $L_1 = L_2 = L_3 = L_4 = L$ [19-21]. When switch M is on, the four inductors will be in series and get charged up by the input source voltage through switching ON S_3 and S_6 as observed in Figure 3(a), whereas the output across filter capacitance is the output voltage fed to the battery. The average voltage across the inductor is $V_L = \frac{V_{in} - V_{out}}{4}$ [22]. When the switch M is OFF, the four inductors will be in parallel to load by switching ON S_1, S_2, S_4, and S_5 as spotted in Figure 3(b).

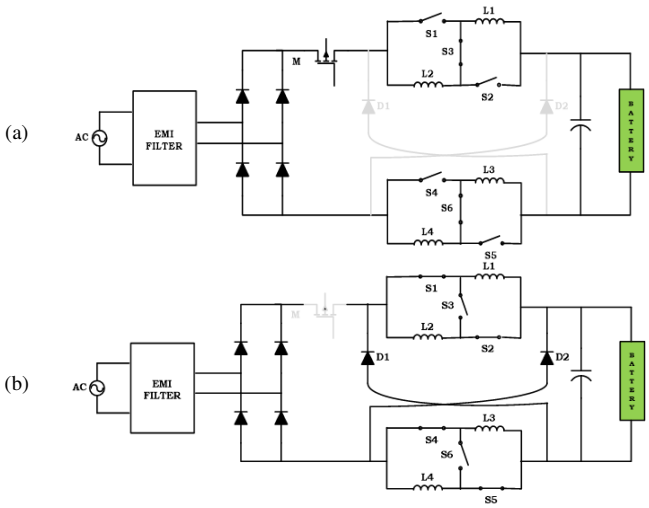

Fig. 3. Switched inductor buck converter current flow when (a) M, S_3, and S_6 are on and (b) M is off and S_1, S_2, S_4, S_5 are on.

The Voltage across the inductor is $V_L = (-V_{out})$ [23]. To derive the voltage gain of the switched inductor hybrid buck converter, the average voltage across the inductor should be equal to zero over a complete period of operation, where the voltage gain is $V_{out}/V_{in} = D/(4\text{-}3D)$ [24]. The proposed PFC switched inductor hybrid buck converter is designed for EVs with 64 V battery. In order to achieve 64 V output voltage with the input voltage of 320 V, the duty ratio is set to $D = 0.5$.

A. Diode Losses in Switched Inductor Buck Converter

The switching frequency of the converter is thought to be 20 kHz with 40 kW output power rating. The inductor current ripple is regarded as 5% and the output voltage ripple as 2% with a maximum output current 0.625 kA. For the calculation of the inductance,

$$L = ((Vin - Vo) * D)/(Fs * \Delta i)$$

Considering Δi=31.3A, the calculated inductance is L = 0.205 mH.

In the mode of discontinuous conduction (DCM), the inductor peak current depends on the duty ratio D [25-26], where T=1/Fs:

$$I_{L,pk} = \frac{V_{in} - V_{out}}{L} DT \quad (2)$$

where V_{in} is the input dc voltage, V_{out} is the output dc voltage, and T is the switching time. The duty ratio each time the inductor discharges current is:

$$D_{off} = \frac{1}{2}\left(\frac{V_{in}}{V_{out}} - 1\right)D \quad (3)$$

which, in the switched inductor buck converter, is half of the traditional conventional buck converter's duty ratio. The overall power loss of the diode is given by:

$$P_d = \frac{L\, I_{Lpk}^2}{2\, T\, v_{out}} V_d \quad (4)$$

where L = 0.205 mH, I_{Lpk} = 31.3 A, T 0.05 ms, and V_{out}= 64 V. Equation (4) is similar for the standard isolated buck converter. The forward diode voltage V_d = 0.8 V for the switched inductor buck architecture will be marginally lower, because the same current value will be divided across the two diodes as V_d/2. As a result, the diode losses are lower than for the buck architecture. Table I summarizes the comparison.

TABLE I. COMPARISON OF DIODE POWER LOSSES

Total diode power	Isolated buck converter diode power loss	Switched inductor buck converter diode power loss
P_d	21.9665W	10.9832W

B. Conduction Losses in the Inductor

The conduction loss of the inductor depends on the rms current, which is computed in (2) with reference to the DCM peak current [27-28]. Consequently, the winding's inductor conduction losses are:

$$P_L = \frac{T^2 D^3}{3L^2}(V_{in} - V_{out})^2 \frac{1}{2}\left(1 + \frac{V_{in}}{V_{out}}\right) X_L \quad (5)$$

where X_L is the total series reactance of the inductor, equal to $2\pi f L$, f = 1/ T is the frequency of the ac input passing through the inductor given as 50 Hz. The calculated X_L is 64.75 Ω. In the switched inductor buck converter, the reactance is equally distributed throughout the four inductors (R_L/4). To observe the difference of the two different topologies, the traditional standard buck conduction loss $P_{L,conv}$ is divided with (5), which yields:

$$\frac{P_{L,SLH}}{P_{L,conv}} = \frac{4}{1 + \frac{V_{out}}{V_{in}}} \quad (6)$$

The converter voltage gain ranges between $0 < \frac{V_{out}}{V_{in}} < 1$, the conduction loss of the inductor in the standard buck is 4 times that of the switched inductor hybrid converter. Table II summarizes the comparison.

TABLE II. COMPARISON OF INDUCTOR POWER LOSSES

Total inductive power	Isolated buck converter inductor power loss	Switched inductor buck converter inductor power loss
P_L	31.5W	7.8W

III. POWER FACTOR CORRECTION TOPOLOGY

The proposed PFC switched inductor hybrid buck converter employs the Current Control Mode (CCM), which is a straight forward implementation and allows high power factor without any sampling of the input source voltage [29-31]. It is not necessary to use input voltage sensing because the slope of the inductor current is proportional to the source voltage. CCM works and monitors each switching cycle by sensing, detecting, and clamping the inductor current. The direction of the current flowing through the inductor during every switching cycle is portrayed in Figure 4. The inductor current is measured and compared to a reference value minus a slope adjustment ramp. The switch is turned off and clamps the current, if the detected current reaches the ramp value. To further enhance the PF in DCM2 (Discontinuous Conduction Mode 2), a scalar normalizing coefficient is additionally used to the value of the slope compensation ramp [32]. If the current cannot reach the value of the compensation ramp, turning off the switch is accomplished by operating it, when the duty ratio reaches its maximum value while operating in DCM1 (Discontinuous Conduction Mode 1).

A. Discontinuous Conduction Mode 1

In DCM1, the topology of the switching duty ratio is fixed as D_{max}, so the mean input current expressed as a function of the angle θ is given as:

$$i_{i,DCM1}(\theta) = D^2 \max \frac{V_{in}|sin\,\theta| - V_{out}}{2L_{on}fs} \quad (7)$$

The input line voltage amplitude V_{in} is 320 V, and the switching frequency fs is 20 kHz. The input current is proportional to the difference between the input voltage and the output voltage. The current only flows when the input voltage exceeds the output voltage. For D = 0.5, it is estimated that V_{out}= 64 V. Without the DCM1, the phase of the current loses its sinusoidal shape. Current conducts whenever, V_{im} (320 V) > V_{out} (64 V). To avoid the PF problem, the switching operation is performed as shown in Figure 4.

B. Discontinuous Conduction Mode 1

In DCM2, the duty ratio is calculated based on ramp and the converter operation condition, so that the input current is:

$$i_{i,DCM2}(\theta) = \frac{I_{ref}^2 L_{on} f_s}{2} \frac{V_{im}|sin\,\theta| - V_{out}}{[V_{im}|\sin\theta| - (1+2k_s)V_{out}]^2} \quad (8)$$

The maximum switching duty ratio is configured as 0.8. Various k_s values from 0.5 to 1 are considered and mathematically analyzed using MATLAB. In general k_s = 1 demonstrates the ideal PF and THD effectiveness. Half a cycle of the input voltage with half wave symmetry are deployed. In the switched inductor hybrid buck converter, the reference voltage should always be less than the peak of the input voltage. The converter runs in DCM1 mode between t_0 and t_1 because the reference voltage is greater than the input voltage.

In $[t_1, t_2]$, the converter runs in DCM2 mode, which means that the current conducts with switching even if $V_{im} < V_{out}$, and this is repeated for $[t_2 - t_3]$. The controller handles the switchover from CCM to DCM mode and vice versa, ensuring seamless transitions every quarter of a cycle.

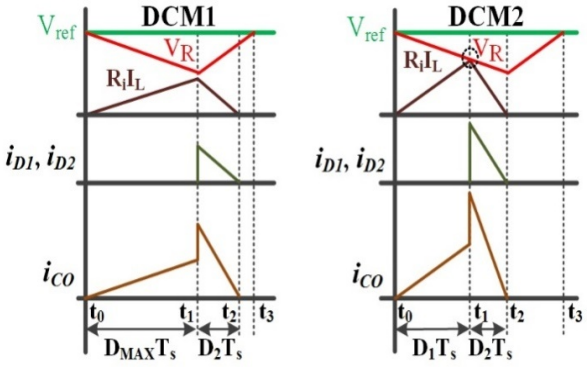

Fig. 4. Switched inductor buck converter current control mode.

The control algorithm with respect to the input voltage, output voltage, and SOC for an isolated hybrid converter, controls the input, and adjusts dc-link voltages. The input values are calibrated to k_p, ki gains, giving rise to minimum tracking error when employing PI controllers. Two PI controllers are used to regulate the ac components (i_d, i_q) as well as the voltage across the dc connection. The internal current regulation loop controls the current, whereas the outside voltage control loop controls the dc link voltage. To determine a PF, the reference value for the q axis current (i_q) is adjusted to 0. Initially, all switches are turned off, and the bulk capacitor is precharged with the anti parallel diodes and an inrush limiting resistor. The inner current loop creates a duty ratio, which ensures that an average inductor current is traced correctly. The outer part of the voltage looping process adjusts the voltage at the dc link by adjusting its input current amplitude. The PI controller is utilized to modify the voltage that controls the loop's gain. The frequency of the crossover should be set to ensure that the dc-link voltage ripple at the double line's frequency is minimal. Finally, feed-forward control logic is employed to calculate the duty ratio. The in-phase current source within the internal control loop results in a PF that is close to 1 and lower input current THD.

IV. CHARGING CURRENT CONTROL TOPOLOGY

The on-board chargers are capable of charging the battery with a household grid load. However, the car's capacity is limited to 240-300 Wh/mile. Fast-charging alternatives are required for cars that have to make additional journeys outside their normal route. Chargers having a power output below 3.3 kW with 1-phase are referred to as slower chargers as well as output 1 chargers with a 120 V outlet. They can be included into the vehicle's engine (on-board) or used for a wall-mounted charging outlet. Level 1 chargers have extended charging times: 5-12 h for 2.1 kW hybrid EV battery capacity of 4-16 kWh and 9-256 h for 2.1 kW EV battery capacity of 15-49 kWh. Level 2 chargers are capable of charging both 3-phase and 1-phase EV batteries up to 21.5 kW [20]. Level 2 chargers, like Level 1 chargers, can be integrated within the car or located outside as specialized EVSE. Level-2 chargers provide three charging time scenarios: 2-5 h for 5 kW with hybrid EV battery capacity of 6-16 kWh, 1-2 h for 18.9 kW with EV capacity of 2-40 kWh and 3-7 h for 9 kW with EV battery capacity of 17-29 kWh [20]. Fast charging converters enable the creation of Level-2 chargers.

The advancement of fast-charging converters encourages the shift to the utilization of EVs. Charging strategies are critical in determining the general effectiveness of the EVs. Fast-charging converters create hurdles for the EV technology, including power loss and battery temperature issues. The primary cause of the capacity loss with cycle count is their stabilization over the usage time. The solid electrolyte interface's passivation layer growth and consolidation create a more stable interface that lowers the rate of corrosion. But again, oxidation is the primary issue of the positive electrode during the storage phase. Charging time at higher SOC is the dominant factor which affects the oxidation properties, causing the power capability to decline and the internal resistance to rise [33-35]. An efficient charger for battery packs charges the battery pack securely and efficiently, while also meeting international standards like IEEE 1547. Conventional charging techniques attempt to charge the battery with the non-linear characteristic. Hence, the proposed isolated hybrid buck converter charges the battery with 3 different protocols: (1) Linearly Declining Current (LDC), (2) pulse charge, and (3) current limiting. The SOC of the battery is determined by the Coulomb counting technique:

$$SOC(t) = SOC(t\text{-}1) + (\int i(t)dt) / \text{nominal capacity} \quad (9)$$

From (1), the age of the battery is divided into 3 stages. In the first stage, the LDC charging strategy is applied. This reduces charging current 0.2 C times based on the battery pack SOC from 0% to 20%. For LDC charging, the initial SOC is going to be taken into consideration. In the second stage, using pulse current, a battery is able to be charged quickly and efficiently with a charging rate of 4 C, if the SOC is between 20% and 80%. The disadvantage is that quick-charging might harm the battery's health when the SOC exceeds 80%. In the third stage, if the SOC is more than 80%, charging currents are applied. In this stage, the battery charging current should be reduced by 50%. Control of the current based on SOC has been performed with the PI loop. With the proposed on-board charger with the isolated hybrid buck converter, the SOL of the battery was improved by 1.3 times. With the current limits applied while in high SOC, the temperature of the battery will be stable.

TABLE III. SWITCHED INDUCTOR HYBRID BUCK CONVERTER COMPONENT PARAMETERS FOR SIMULATION ANALYSIS

Component parameters	Value
Input DC Voltage	320 V
Output DC Voltage	64 V
Switching frequency	20 KHz
Switched inductor hybrid buck inductor	0.205 mH
Switched inductor hybrid buck capacitor	3.91 mF

V. SIMULATION RESULTS

In Figure 5, the isolated buck converter engages a transformer with turns ratio of 3:1, resulting in more losses. Figure 6(a) displays the input ac voltage of 320 V rms given to the isolated converter and the output voltage of 62.3 V dc. The input ac is not sinusoidal. Figure 6(b) exhibits the THD of the input AC current with the fundamental frequency of 50Hz.

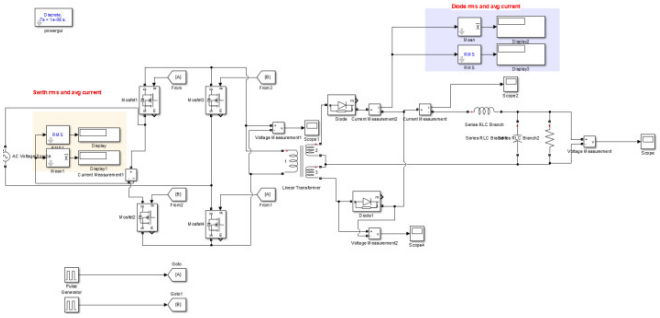

Fig. 5. Simulated isolated converter designed in Matlab/Simulink.

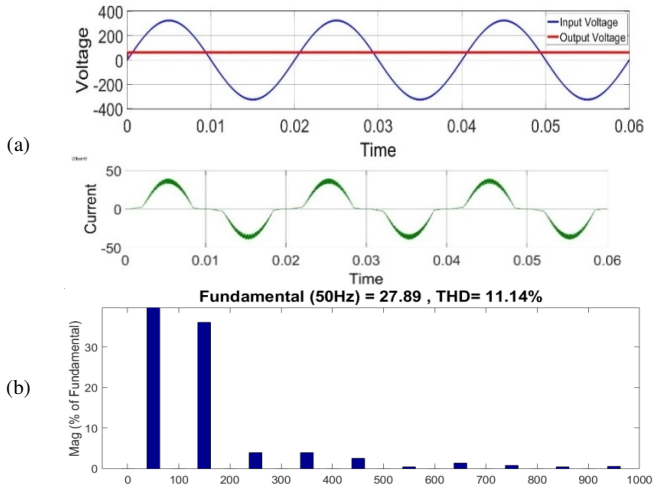

Fig. 6. (a) Isolated converter input voltage, input current, and output voltage, (b) isolated converter THD of input current.

Figure 7(a) presents the design of the proposed switched inductor hybrid buck converter. In Figure 7(b), the control algorithm of the switched inductor hybrid buck non-isolated converter is designed. The control algorithm takes reference of the shape of the input voltage, the input current, and the charging current limits based on SOC.

Figure 8(a) shows the input AC voltage of 320 V rms given to the switched inductor hybrid buck non-isolated converter and the output voltage of 64V DC. The input AC current is sinusoidal. Figure 8(b) depicts the THD of the input AC current with the fundamental frequency of 50 Hz. The THD of the switched inductor hybrid buck non-isolated converter is less than 5.

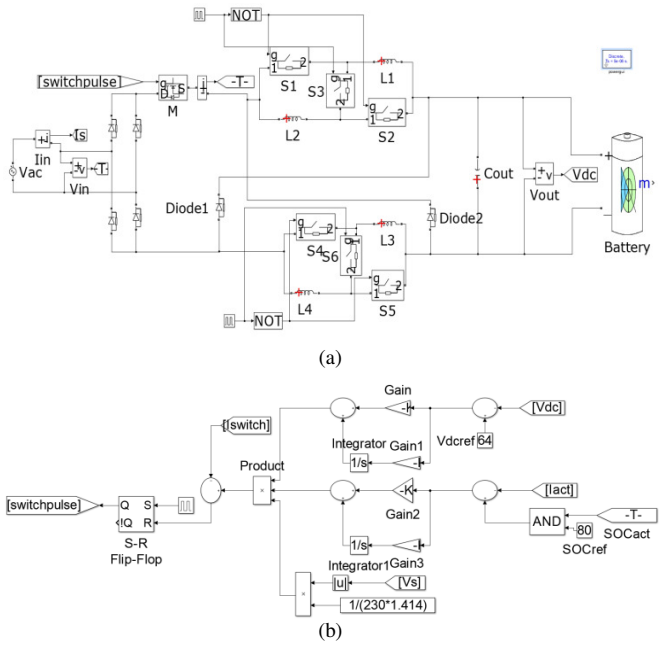

Fig. 7. (a) Simulated switched inductor hybrid buck non-isolated converter, (b) simulated PI-based controlled logic.

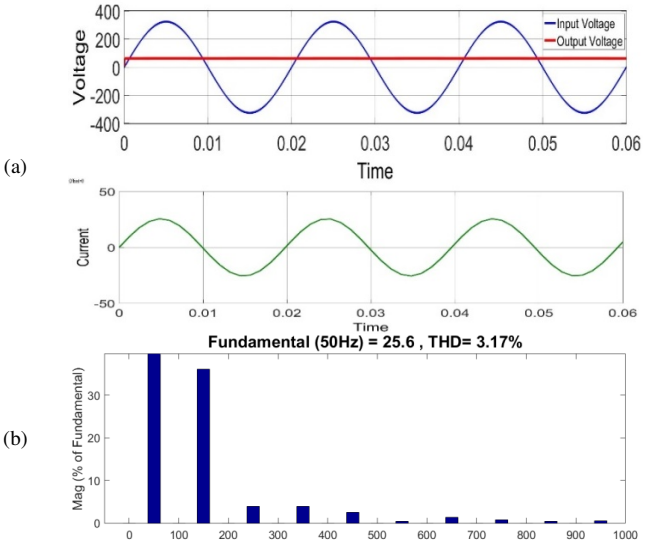

Fig. 8. (a) Switched inductor hybrid buck non-isolated converter input voltage, input current, and output voltage, (b) switched inductor hybrid buck non-isolated converter THD of the input current.

In Figure 9(a), it can be noticed that changing SOC from 70% to 80% took around 350 s. After reaching 80%, the charging current limits were applied, the charging current was reduced by 50%, and hence the rate of charging slowed down. With the charging current limits applied at higher SOC values, the battery temperature did not increase, so the battery life of the improved. The activation of the current limits is spotted in Figure 9(b). Figure 10 illustrates the calculated losses of the isolated and switched inductor hybrid buck non-isolated converters.

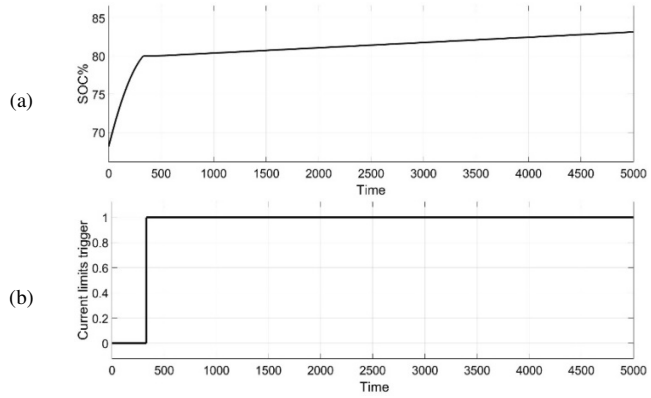

Fig. 9. (a) Battery SOC of the switched inductor hybrid buck non-isolated converter, (b) current limit activation from the control logic.

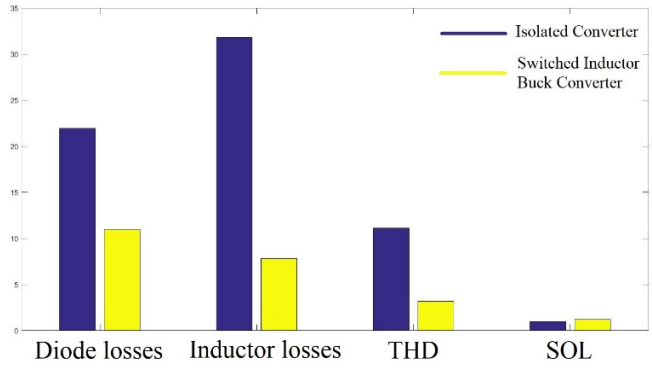

Fig. 10. Calculated losses of the isolated and the switched inductor hybrid buck non-isolated converter.

As demonstrated in Table I, the diode losses of the isolated buck converter are 21.96 W and the diode losses of the switched inductor buck converter are 10.98 W. The inductor losses (Table II) of the isolated buck converter are 31.96 W and of the switched inductor buck converter are 7.8 W. From Figure 6(b) and Figure 8(b), it is noted that the THD of the switched inductor buck converter is less. With the charging limits applied, the SOL of the battery is improved by 1.2 times, proving that the switched inductor hybrid buck converter is efficient for on-board chargers.

VI. CONCLUSION

A non-Isolated buck PFC converter suitable for application to electric vehicle chargers, with switched inductor and using controlled current mode was introduced, analyzed, and verified with simulations. The method for implementing the current controlled mode and selecting the k_s ramp value was presented. Mathematical analysis revealed that the switched inductor buck converter topology has overall losses above all the inductor conduction losses compared to the isolated buck converter. The 60 W simulated model was tested, and the efficiency of the non-isolated buck converters was always larger than that of the traditional isolated buck converters. These findings support the effectiveness and high efficiency of the non-isolated switching inductor buck converter as an electric vehicle charger application.

FUTURE WORK

This work can be also extended to other types of chargers, for the correction of the power factor in order for the EVs to have better efficiency and battery life.

ACKNOWLEDGEMENT

The authors wish to thank the management of Electrical and Electronics Engineering Department of Koneru Lakshmaiah Education Foundation for their kind support.

REFERENCES

[1] A. S. Daniel and K. R. M. V. Chandrakala, "Design of an Isolated Onboard Plug-in Electric Vehicle Charger," in *7th International Conference on Electrical Energy Systems*, Chennai, India, Feb. 2021, pp. 147–149, https://doi.org/10.1109/ICEES51510.2021.9383717.

[2] N. D. Dao and D.-C. Lee, "Modulation of Bidirectional AC/DC Converters Based on Half-Bridge Direct-Matrix Structure," *IEEE Transactions on Power Electronics*, vol. 35, no. 12, pp. 12657–12662, Dec. 2020, https://doi.org/10.1109/TPEL.2020.2994776.

[3] A. Pandey and S. Pattnaik, "Design and Analysis of Extendable Switched-Inductor and Capacitor-Divider Network Based High-Boost DC-DC Converter for Solar PV Application," *IEEE Access*, vol. 10, pp. 66992–67007, 2022, https://doi.org/10.1109/ACCESS.2022.3185107.

[4] A. Rajabi, A. Rajaei, V. M. Tehrani, P. Dehghanian, J. M. Guerrero, and B. Khan, "A Non-Isolated High Step-Up DC-DC Converter Using Voltage Lift Technique: Analysis, Design, and Implementation," *IEEE Access*, vol. 10, pp. 6338–6347, 2022, https://doi.org/10.1109/ACCESS.2022.3141088.

[5] A. Mirzaei, M. Rezvanyvardom, and E. Najafi, "A fully soft switched high step-up SEPIC-boost DC-DC converter with one auxiliary switch," *International Journal of Circuit Theory and Applications*, vol. 47, no. 3, pp. 427–444, 2019, https://doi.org/10.1002/cta.2595.

[6] H. N. Chavan and R. Wandhare, "High Voltage Gain DC-DC Non-Isolated Converter with Generalized Stages," in *9th Power India International Conference*, Sonepat, India, Feb. 2020, pp. 1–6, https://doi.org/10.1109/PIICON49524.2020.9112977.

[7] J. Marjani, A. Imani, A. Hekmati, and E. Afjei, "A new dual output DC-DC converter based on SEPIC and Cuk converters," in *International Symposium on Power Electronics, Electrical Drives, Automation and Motion*, Capri, Italy, Jun. 2016, pp. 946–950, https://doi.org/10.1109/SPEEDAM.2016.7525949.

[8] J. Ahmad, M. D. Siddique, A. Sarwar, C. H. Lin, and A. Iqbal, "A high gain noninverting DC–DC converter with low voltage stress for industrial applications," *International Journal of Circuit Theory and Applications*, vol. 49, no. 12, pp. 4212–4230, 2021, https://doi.org/10.1002/cta.3129.

[9] J. Zhao and D. Chen, "Switched-Capacitor High Voltage Gain Z-Source Converter With Common Ground and Reduced Passive Component," *IEEE Access*, vol. 9, pp. 21395–21407, 2021, https://doi.org/10.1109/ACCESS.2021.3054880.

[10] J. Kathiresan, S. K. Natarajan, and G. Jothimani, "Design and implementation of modified SEPIC high gain DC-DC converter for DC microgrid applications," *International Transactions on Electrical Energy Systems*, vol. 31, no. 8, 2021, Art. no. e12921, https://doi.org/10.1002/2050-7038.12921.

[11] K. Sundaramoorthy, "Switched Inductor-Capacitor Network Based Non-Isolated DC-DC Converter: A Double2 Gain Converter with Single Switch," in *National Power Electronics Conference*, Tiruchirappalli, India, Dec. 2019, pp. 1–6, https://doi.org/10.1109/NPEC47332.2019.9034827.

[12] M. A. Salvador, J. M. de Andrade, T. B. Lazzarin, and R. F. Coelho, "Nonisolated High-Step-Up DC–DC Converter Derived from Switched-Inductors and Switched-Capacitors," *IEEE Transactions on Industrial*

Electronics, vol. 67, no. 10, pp. 8506–8516, Oct. 2020, https://doi.org/10.1109/TIE.2019.2949535.

[13] M. A. Salvador, J. M. de Andrade, T. B. Lazzarin, and R. F. Coelho, "Methodology for synthesis of high-gain step-up DC–DC converters based on differential connections," *International Journal of Circuit Theory and Applications*, vol. 49, no. 2, pp. 306–326, 2021, https://doi.org/10.1002/cta.2892.

[14] N. Elsayad, H. Moradisizkoohi, and O. A. Mohammed, "A Single-Switch Transformerless DC–DC Converter With Universal Input Voltage for Fuel Cell Vehicles: Analysis and Design," *IEEE Transactions on Vehicular Technology*, vol. 68, no. 5, pp. 4537–4549, May 2019, https://doi.org/10.1109/TVT.2019.2905583.

[15] J. Gnanavadivel, K. Jayanthi, S. Vasundhara, K. V. Swetha, and K. Jeya Keerthana, "Analysis and design of high gain DC-DC converter for renewable energy applications," *Automatika*, vol. 64, no. 3, pp. 408–421, Jan. 2023, https://doi.org/10.1080/00051144.2023.2170062.

[16] H. Komurcugil, N. Guler, S. Bayhan, and O. Gulbudak, "Hysteresis Current Control of Buck-Boost Non-Isolated Onboard Charger for Electric Vehicles," in *49th Annual Conference of the IEEE Industrial Electronics Society*, Singapore, Singapore, Oct. 2023, pp. 1–6, https://doi.org/10.1109/IECON51785.2023.10312657.

[17] N. Somboonpanya, S. Khomfoi, and T. Phophongviwat, "Non-isolated Onboard EV Charger Controller Design Based on Port-Hamiltonian Approach," in *Transportation Electrification Conference and Expo, Asia-Pacific*, Chiang Mai, Thailand, Dec. 2023, pp. 1–4, https://doi.org/10.1109/ITECAsia-Pacific59272.2023.10372304.

[18] K. S. Raja Sekhar, M. A. Chaudhari, and R. Kumar, "A Non-isolated Two Port Converter for Battery charging and Auxilary supply applications," in *Renewable Energy and Sustainable E-Mobility Conference*, Bhopal, India, May 2023, pp. 1–5, https://doi.org/10.1109/RESEM57584.2023.10236027.

[19] J. Soldado-Guaman, V. Herrera-Perez, S. Z. Djokic, R. Isa-Jara, E. Guevara-Cabezas, and J. Hernandez-Ambato, "Comparison of Isolated and Non-Isolated Multiple Input - Single Output DC-DC Converters for Low-Power Renewable Sources Integration," in *Green Technologies Conference*, Denver, CO, USA, Apr. 2023, pp. 101–106, https://doi.org/10.1109/GreenTech56823.2023.10173840.

[20] A. Singh, J. Gupta, and B. Singh, "A Single-Stage Isolated High Power Factor AC-DC Converter based Battery Charger for Light Electric Vehicles," in *10th Power India International Conference*, New Delhi, India, Nov. 2022, pp. 1–6, https://doi.org/10.1109/PIICON56320.2022.10045128.

[21] A. Jha and B. Singh, "Portable Battery Charger for Electric Vehicles," in *International Conference on Sustainable Energy and Future Electric Transportation*, Hyderabad, India, Jan. 2021, pp. 1–6, https://doi.org/10.1109/SeFet48154.2021.9375782.

[22] B. Singh and J. Gupta, "Improved Power Quality On-Board Charging Solution for Light Electric Vehicles," in *Transportation Electrification Conference & Expo*, Chicago, IL, USA, Jun. 2021, pp. 462–467, https://doi.org/10.1109/ITEC51675.2021.9490189.

[23] U. Sharma and B. Singh, "An Onboard Charger for Light Electric Vehicles," in *International Conference on Power Electronics, Drives and Energy Systems*, Jaipur, India, Dec. 2020, pp. 1–6, https://doi.org/10.1109/PEDES49360.2020.9379743.

[24] U. Sharma and B. Singh, "A Non-isolated Onboard Charger for Electric Vehicle," in *Transportation Electrification Conference & Expo*, Chicago, IL, USA, Jun. 2021, pp. 446–451, https://doi.org/10.1109/ITEC51675.2021.9490193.

[25] T. Gherman, D. Petreus, T. Patarau, and A. Ignat, "A study of an Electrical Vehicle Battery Charger's DC-DC Stage," in *41st International Spring Seminar on Electronics Technology*, Zlatibor, Serbia, May 2018, pp. 1–6, https://doi.org/10.1109/ISSE.2018.8443658.

[26] O. Turksoy, U. Yilmaz, and A. Teke, "Overview of battery charger topologies in plug-in electric and hybrid electric vehicles," in *16th International Conference on Clean Energy*, Famagusta, N. Cyprus, May 2018, pp. 1–8.

[27] A. Khaligh and M. D'Antonio, "Global Trends in High-Power On-Board Chargers for Electric Vehicles," *IEEE Transactions on Vehicular Technology*, vol. 68, no. 4, pp. 3306–3324, Apr. 2019, https://doi.org/10.1109/TVT.2019.2897050.

[28] M. Yilmaz and P. T. Krein, "Review of Battery Charger Topologies, Charging Power Levels, and Infrastructure for Plug-In Electric and Hybrid Vehicles," *IEEE Transactions on Power Electronics*, vol. 28, no. 5, pp. 2151–2169, May 2013, https://doi.org/10.1109/TPEL.2012.2212917.

[29] S.-G. Jeong, J.-M. Kwon, and B.-H. Kwon, "High-Efficiency Bridgeless Single-Power-Conversion Battery Charger for Light Electric Vehicles," *IEEE Transactions on Industrial Electronics*, vol. 66, no. 1, pp. 215–222, Jan. 2019, https://doi.org/10.1109/TIE.2018.2826458.

[30] T. Soong and P. W. Lehn, "On-board Single-Phase Electric Vehicle Charger with Active Front End," in *International Power Electronics Conference (IPEC-Niigata 2018 -ECCE Asia)*, Niigata, Japan, May 2018, pp. 3203–3208, https://doi.org/10.23919/IPEC.2018.8507547.

[31] A. V. J. S. Praneeth, D. Vincent, and S. S. Williamson, "An Universal On-board Battery Charger with Wide Output Voltage Range for Electric Transportation," in *IEEE Energy Conversion Congress and Exposition*, Baltimore, MD, USA, Sep. 2019, pp. 1159–1165, https://doi.org/10.1109/ECCE.2019.8912749.

[32] R. W. Erickson and D. Maksimovic, *Fundamentals of Power Electronics*, 2nd Edition. New York, NY, USA: Kluwer Academic Publishers, 2004.

[33] K. Unni and S. Thale, "Energy Consumption Analysis for the Prediction of Battery Residual Energy in Electric Vehicles," *Engineering, Technology & Applied Science Research*, vol. 13, no. 3, pp. 11011–11019, Jun. 2023, https://doi.org/10.48084/etasr.5868.

[34] N. T. Diep and N. K. Trung, "Transmitting Side Power Control for Dynamic Wireless Charging System of Electric Vehicles," *Engineering, Technology & Applied Science Research*, vol. 12, no. 4, pp. 9042–9047, Aug. 2022, https://doi.org/10.48084/etasr.4988.

[35] M. E. Bendib and A. Mekias, "Solar Panel and Wireless Power Transmission System as a Smart Grid for Electric Vehicles," *Engineering, Technology & Applied Science Research*, vol. 10, no. 3, pp. 5683–5688, Jun. 2020, https://doi.org/10.48084/etasr.3473.